ISSN PRINT 2319 1775 Online 2320 7876

Research paper UGC CARE Listed (Group -I) Journal Volume 11,S Iss 3, Dec 2022

DEVELOPMENT AND EVALUATION OF BETULINIC ACID CO-DELIVERED FEMARA LOADED DAMMAR GUM NANOPARTICLES TO FIGHT CANCER CELL LINE

Vijeta Kumari*, Dr. Sanjeev Sharma
Department of Chemistry, Om Sterling Global University, Hisar-125001, Haryana, India.
vijeta.p7@gmail.com
sanjeev075@gmail.com

ABSTRACT
Chemotherapeutics approaches used to cure cancer are frequently faced a problem of drug resistances. Secondary metabolites of plants having anticancer potency can be effectively raised by formulating them at nanoscale. Betulinic acid (BA) is a pentacyclic triterpenoid molecule that has a potency to kill cancer cells by interfering in cellular proliferation. Femara (FEM) is an adjuvant molecule used to specially treat breast cancer. It is chemically known as Letrozole. To improve the bioavailability and to generate synergetic effect, BA and FEM loaded dammar gum nanoparticles (BFDNPs) were synthesized by oil in oil (O/O) emulsion solvent evaporation techniques. The zeta potential value of BFDNPs was come out to be -45.9 mV representing relative stability of nanoparticles. The percentage encapsulation efficiency value was found to be 72.5% for BA and 76.6% for FEM. The BFDNPs possess particle size in the range of 45 – 55nm as revealed by TEM. The BFDNPs exhibited sustained release and their anti-oxidant and anti-cancer potency was much more pronounced than free BA and FEM particles alone. The *in vitro* studies demonstrated that BA and FEM encapsulated in dammar gum inhibited growth of MCF-7 cell lines more effectively than BA and FEM alone which proved their robust anticancer potential.

Keywords: Dammar gum, Betulinic acid, Femara, Anti-cancer, Nanoparticles

INTRODUCTION
Nanotechnology in cancer treatment opens a new emerging area of pharmaceutical findings. Nanosized drug molecules provides novel highly potent bioactive loaded nanoplatform to fight cancer cells. Chemotherapy is frequently utilized to manage various cancers [1]. In contrast, these conventional curative approaches are linked to brutal effects, particularly drug tolerance or resistance [2, 3]. Nanotechnology enabled solutions for life-threatening diseases are popular now-a-days. The bioactive agents at nanometric scale exhibit high bioavailability at low dose and enhanced antioxidant and anticancer potential. In USA, National Institute of Cancer has

ISSN PRINT 2319 1775 Online 2320 7876

Research paper UGC CARE Listed (Group -I) Journal Volume 11,S Iss 3, Dec 2022

promoted the examination of the antitumor effect of many secondary metabolites of plants [4, 5]. Phytochemicals like boswellic acid and Betulinic acid (BA) have already reported in literature to exert cytotoxic effects [6]. Contemporary studies have shown that the morphological properties of nanoparticles are extremely important for attaining anticancer activity with less side effects [7].The size, shape & surface traits of nanoparticles influence the pharmacokinetic as well as pharmacodynamic properties of nanoparticles.

BA (pentacyclic triterpenoid) occurs either as aglycone of saponins or as free carboxylic acid [8]. In its presence, glucocorticoid receptors get transformed leading to the reduction of Bcl2 (anti-apoptotic proteins) in breast cancer cell lines (Michigan Cancer Foundation-7) of humans [9, 10]. Due to its low level of toxicity, BA is generally used in pharmaceutical formulations that could be administered both orally & topically [11, 12].

Biodegradability & biocompatibility are ideal features considered for selection of an agent for encapsulating numerous drugs [13, 14]. Dammar gum is a novel encapsulation compound employed for therapeutic action and has shown proportional augmentation in encapsulation efficiency with increase in gum concentration [15].

Femara (FEM) is a new orally active, potent and selective aromatase inhibitor for the hormonal treatment of advanced breast cancer in postmenopausal women and used to treat breast cancer [16, 17]. It is a nonpolar molecule which acts by blocking the enzyme aromatase, which turns the hormone androgen into small amounts of estrogen in the body. [18-19]. Its structural specificity with the cell membrane and adjuvant hormonal therapy provides anticancer activity [20].

In the present study, BA co-delivered FEM polymeric nanoplatform were prepared with the aim to improve bioavailability, bring synergism and to overcome the side effects. The encapsulation of FEM and BA in the polymeric nanoparticles renders sustained release & higher therapeutic efficacy at low dosage.

Materials and Methods

Materials

Gum dammar was purchased from MP Biomedicals, LLC, France. Betulinic acid (>90%) and Femara were procured from Sigma Aldrich, India. Cell line MCF-7-Human breast adenocarcinoma cells was procured from National Centre for Cell Science (NCCS), Pune. All the chemicals used in the present study were of analytical grade.

Preparation of BA & FEM loaded dammar gum nanoparticles (BFDNPs)

The BFDNPs were synthesized by oil in oil emulsion solvent evaporation method [21]. 200 mg of dammar gum, 60mg of BA and 8mg of FEM were dissolved in 100ml of propanol. 25 mg of Magnesium stearate was added to the above solution, and the resulting mixture was kept under magnetic stirring (800 rpm) for 30min. 60 ml of liquid paraffin oil was poured slowly to the

ISSN PRINT 2319 1775 Online 2320 7876

Research paper UGC CARE Listed (Group -I) Journal Volume 11,S Iss 3, Dec 2022

mixture with continuous stirring at 800 rpm at 40˚ C for 10h and centrifuged at 8800 rpm, 4°C for 40 minutes. The pellet was isolated and suspended in cryoprotectant (D-Mannitol, 5% w/v) and freeze-dried.

Characterization of synthesized BFDNPs

Zetasizer Nano ZS-90 was used to assess the average size and size distribution (polydispersity index) of optimized nanoformulation of BFDNPs. After centrifugation at 8800 rpm (4˚C) for 40 minutes, the supernatant having the unbound drug was collected and analyzed by HPLC and encapsulation efficiency was calculated using following formula:

Percent Entrapment efficiency = (Total Drug-Unbound Drug/Total Drug) × 100

The size and morphology of optimized batch of BFDNPs was analyzed by transmission electron microscope. The FTIR analysis of BA, FEM, dammar Gum and BFDNPs was analyzed by Fourier transform infrared spectrophotometer in range of 4500–500 cm^{-1}.

In vitro release profile of BFDNPs

The dialysis sac method was used to study the release profile. 10 mg of BA co-delivered FEM loaded dammar gum nanoparticles were transferred to dialysis sac and positioned in water (10ml) and immersed in ethanol (25%) - phosphate buffer (0.1 M) saline pH 7.4 and constantly stirred at 100 rpm at a steady temperature of 37 °C [21]. One ml sample was withdrawn and collected at regular intervals of 1, 2, 3, 6, 12, and 24 h and examined by HPLC BA (210.7 nm, 6.43 min, FEM (256 nm, 7.89 min).

Antioxidant activity

The antioxidant potential of BA, FEM, Dammar Gum and BFDNPs was evaluated by 1,1-diphenyl-2-picrylhydrazyl (DPPH) assay [22]. DPPH is a free radical was homogenously mixed in methanol (3.9 mg/100 ml). Pure BA, FEM, Dammar Gum and BFDNPs were incubated along with DPPH for 30 min in dark condition to evaluate the inhibition of DPPH in triplicate run and the absorption peak was recorded using UV spectrophotometer at 517 nm. Blank dammar NPs were treated as a negative control while pure Betulinic acid and FEM were used as positive control. The percentage inhibition of DPPH by pure BA, FEM and BFDNPs was calculated by formula as under:

$$\text{Percent antioxidant activity} = \frac{\text{Absorbance of control- Absorbance of sample}}{\text{Absorbance of control}} \times 100$$

In-vitro assay for cytotoxic activity (MTT assay)

Cell lines (both normal and cancer) were raised in media supplemented with inactivated FBS (10%) solution, antibiotic streptomycin 80µl/ml with 80µl/ml penicillin concentration, incubated at 37^0C temp, 5%CO_2 enviorment [21, 23]. After attaining 75% confluence, 0.25% trypsin solution were used for subcultured in laminar air flow under sterile conditions. The seeding of cells was experimented in 96 – well plates (10^4 per 100µl per well).The growth characteristics

ISSN PRINT 2319 1775 Online 2320 7876

Research paper UGC CARE Listed (Group -I) Journal Volume 11,S Iss 3, Dec 2022

pattern was analyzed to evaluate density of each cell line. For optimization the wells were treated after 8 h incubation with various concentration of BFDNPs (0.1-500µg/ml) & Betulinic acid for three days (in triplicate). Subsequently, after raising cells, the medium was replaced by 3µl of MTT solution (5mg/ml) and incubated for 3 h. The percent of metabolically active cells were compared with untreated controls on the basis of the mitochondrial conversion of 3-(4, 5-dimethylthiazol-2-yl) 2, 5 diphenyltetrazolium bromide (MTT) to Formazan crystals. The formazan crystals were dissolved in DMSO and its absorbance was calculated by 96 wells microplate reader at 570 nm. The anticancer activity of BFDNPs was evaluated using pure BA and FEM as standard by MTT assay against cell line MCF-7 (human breast adenocarcinoma cells). The percentage cell growth inhibition (1) and percentage cytotoxicity (2) was calculated by following formula:

%viability = $(A_{Tr} – A_{Bl}) / (A_{Ct} – A_{Bl}) \times 100$ ……. (1)

Where A_{Tr} = Absorbance for treated cells (drug); A_{Bl} = Absorbance for blank

A_{Ct} = Absorbance for control (untreated)

%cytotoxicity = 100 – Percent cell survival (%) ……. (2)

Results and Discussion

Particle size and Zeta Potential

The BFDNPs were analyzed for particle size and zeta potential. The BFDNPs size was found to be 240.9 nm (Fig 1) with zeta potential value of -45.9 mV (Fig 2), signifying relative stability of prepared nanoformulation.

Encapsulation efficiency

The percentage encapsulation efficiency value depends upon the structure of molecule, type of technique involved, the chemical nature of encapsulating materials and dielectric constant of medium of nanoparticles synthesis [21, 24]. The percentage encapsulation efficiency was calculated using HPLC analysis of supernatant having unbound drug in order to determine the percent of bound drug and was found to be 72.6% for BA and 77.1 % for FEM (Fig 5). BA and FEM are non-polar hydrophobic in nature. They are greatly soluble in gum solution synthesized in propanol. Due to hydrophobic nature of dammar gum, there was a high affinity between gum, BA and FEM. This same nature affinity resulted in increased encapsulation efficiency of the drug in dammar gum.

Morphological characterization of* BFDNPs *by SEM

The BFDNPs were segregated and uniformly spherical with size range of 40 – 58 nm as revealed by Transmission Electron Microscopy (Figure 3). A variation in size was experimentally found in the nanoparticles evaluated through PSA and SEM. This is because PSA works on the principal of fluidized ionic surrounding of the nanoparticles, whereas TEM based on the

ISSN PRINT 2319 1775 Online 2320 7876

Research paper UGC CARE Listed (Group -I) Journal Volume 11,S Iss 3, Dec 2022

principle of the particle dimension in the isolated dried atmosphere leading to shrinkage of particle. The size dimension of nanorange particles affects drug release rate [25, 26]. NPs undergo distribution to different concentration to various body organs according to their shape & size. The relative stability, biocompatibility with natural body environment and penetration of nanoparticles inside the cell plasma membrane are likewise governed by morphology & size of nanoparticles [26]. Nanoparticles having small size range are maintained in systemic circulation for an longer period in comparison to large size nanoparticles [27].

FTIR Analysis of Drug Samples

The FTIR spectroscopy is used to study both the interaction [27] and evaluation of the nanoencapsulation of bioactive molecules [28]. The FTIR spectra of pure drug BA, FEM, dammar gum and BFDNPs is shown in Figure 4. The FTIR spectrum of BA showed absorption peak bands at 3440 cm $^{-1}$ for the -OH and 2928.0 cm $^{-1}$& 2359 cm $^{-1}$ for the terminal –CH_3 groups. The FTIR spectrum of FEM in Figure 4 B showed characteristic absorption band for =C-H stretching at 2942 cm $^{-1}$and 1598 cm $^{-1}$ for C=C ring stretching. The value of wave number at 1465 cm $^{-1}$ and 3389 cm $^{-1}$signified -NH_2stretch. The FTIR spectrum of dammar gum in Figure 4 C showed the FTIR peak at 3428cm $^{-1}$for –OH stretch and peak at 2926 cm $^{-1}$indicate aliphatic –CH stretch of dammar gum. Figure 4 D representing the FTIR spectrum of BFDNPs showed variations between wave numbers 3372 cm^{-1}, 1418 cm $^{-1}$,2348 cm $^{-1}$and 2982 cm^{-1} in BFDNPs. This region is the IR stretching vibration zone of functional groups like–OH, C=C Stretch,-CH_3 Stretch and the C-H stretch. The weak-physical bonds such as dipole-dipole interaction, hydrogen bonding and weak Van der Waals forces take place between the C-H present in the drug molecule and OH present in dammar gum. The drugs & excipients revealed characteristic peaks in FTIR spectrum. The decrease in peak intensity and bands were shifted, confirmed presence of physical interaction among FEM, BA &dammar gum.

In-vitro drug release

The persistent release of bioactive potent molecule out of nanoparticles cage protects it from rapid metabolism and degradation [29]. Figure 5 shows the *in vitro* drug release profile of BA, FEM, and BFDNPs. The *in-vitro* drug release data showed that 92% of the pure BA and 96% of pure FEM was released in 5h only, while the BFDNPs exhibited sustained release of the drug due to high better and efficient entrapments of drug in dammar gum. The BFDNPs showed release of 18% BA and 19.2% FEM after 1 h of administration. After 24 h, 76% of BA and 82% FEM was released from BFDNPs. Overall drug release of BFDNPs showed sustained release profile of BA and FEM with the passage of time which is due to hydrophobic (nonpolar) nature of BA and FEM. Dammar gum also create a thick, strong walled and dense matrix around the BA and FEM particles thus ensuring its sustained release.

ISSN PRINT 2319 1775 Online 2320 7876

Research paper UGC CARE Listed (Group -I) Journal Volume 11,S Iss 3, Dec 2022

HPLC Conditions:
1Equipment Model: Agilent 1200 Infinity Series
2Column: ZORBAX SB C-18,Dimension(mm):150 x 4.6;Particle size(µ):5;
3Detector: DAD
4Pump: Isocratic
5Mobile Phase: Acetonitrile:Water (80:20)
6Flow Rate: 1ml/min
7Wavelength: Betulinicacid (210 nm)
8Injection volume: 2 µl
9Retention Time(min.)Betulinicacid (6.6
HPLC Conditions:
1Equipment Model: Agilent 1200 Infinity Series
2Column: ZORBAX SB C-18,Dimension(mm):150 x 4.6;Particle size(µ):5;
3Detector: DAD
4Pump: Isocratic
5Mobile Phase: Acetonitrile:Water (80:20)
6Flow Rate: 1ml/min
7Wavelength: Betulinicacid (210 nm)
8Injection volume: 2 µl9Retention Time(min.)Betulinicacid (6.67

Anti-oxidant activity

The DPPH analysis is technique is used to evaluate quantitatively the antioxidant potency/activity of encapsulated molecules [31]. DPPH (1,1-diphenyl-2-picrylhydrazyl) is a stable free radical, that contain unpaired electrons that delocalized over the molecule, absorbing light to show excitation and during emission emit a deep violet coloration. It shows absorption near 517 nm [32]. When a DPPH solution is uniformly mixed with a molecule that can donate (oxidizing nature) a hydrogen atom the violet color is disappearance. The BA and FEM are well known antioxidant potency. The solution of antioxidant molecules BA and FEM were incubated with DPPH and a stable non-radical form of DPPH was obtained resulting in the change of violet color to pale yellow. Thus, a decrease in absorbance band was observed. The BA and FEM contain labile hydrogen atoms that liberation leads to inhibit DPPH. The BFDNPs exhibited higher percent inhibition of DPPH as compared to BA and FEM alone due to nanometric dimension with a large surface area during dark incubation that provided protection to BA and FEM from being oxidized (Fig 6).

ISSN PRINT 2319 1775 Online 2320 7876

Research paper **© 2012 IJFANS. All Rights Reserved, UGC CARE Listed (Group -I) Journal Volume 11,S Iss 3, Dec 2022**

Anti-cancer activity

The cytotoxic efficacy of nanoparticles represented in Figure 7, 8 was primarily due to their larger surface area, which enabled highly efficient drug delivery and anticancer potency [33].The nanoparticles of size 100 nm range are better competent to infiltrate tumor cells effortlessly or effectively via retention effect and better vascular permeation [34]. Hence, potency of NPs against the cancer cell lines depends on size [35,36]. The nano range particles can enter deep inside the tumor cells with greater efficiency. In the present study, the anti-cancer activity of BFDNPs was found to be more efficient than pure active drug alone. *In vitro* study showed that BA and FEM encapsulated in dammar gum inhibited the growth of MCF-7 more effectively than the free drugs alone. The IC50 values (µg/ml) of synthesized nanoparticles along with standard drug tamoxifen & Betulinic acid are given in Table 1.The results revealed that BFDNPs showed potent anticancer effect with IC50 of 3.85 µg/ml in comparison to standard drugs FEM and BA alone as analyzed under optical microscope (Fig.10) MCF-7. The potent anticancer action of BFDNPs was primarily due to the combined synergistic effect of FEM and BA in BFDNPs.

CONCLUSIONS

Significant achievements in drugs formulation world leads to open a gate for nanotechnology interventions to address and treat diseases effectively. Nano-drug delivery systems have broad potential to deliver nanoparticles with bigger payloads including dual drug delivery to create synergetic effects of secondary metabolites with drugs at therapeutics size. In spite of the discovery of abundance of anticancer drugs molecules, the major problems of these drug molecules are tolerance/resistance along with low bioavailability as well as low drug residence time in the body. Thus it is important to develop novel nanoformulations consisting more powerful excipients inorder to enhance solubility in water, bioavailability to blood from intestine, therapeutic potential to kill cancer cell lines and to reduced dosage. In the current study, the synergistic antioxidant as well as anticancer potential of novel nanoformulation containing Betulinic acid co-delivered Femara loaded dammar gum nanoparticles based on dual drug delivery approach have emerging as promising molecule to combat cancer effectively.

Conflict of Interest

There is no conflict of interest whatever.

REFERENCES

1. Myers, David J., and Jason M. Wallen. "Lung adenocarcinoma." In StatPearls [Internet]. StatPearls Publishing, 2022.

ISSN PRINT 2319 1775 Online 2320 7876

Research paper UGC CARE Listed (Group -I) Journal Volume 11,S Iss 3, Dec 2022

2. Cocco, S., Leone, A., Roca, M. S., Lombardi, R., Piezzo, M., Caputo, R.,. & De Laurentiis, M. (2022). Inhibition of autophagy by chloroquine prevents resistance to PI3K/AKT inhibitors and potentiates their antitumor effect in combination with paclitaxel in triple negative breast cancer models. Journal of Translational Medicine, 20(1), 1-17.
3. Zhao, B., Li, L., Lv, X., Du, J., Gu, Z., Li, Z.. & Hong, Y. (2022). Progress and prospects of modified starch-based carriers in anticancer drug delivery. Journal of Controlled Release, 349, 662-678.
4. Yuan, M., Zhang, G., Bai, W., Han, X., Li, C., & Bian, S. (2022). The Role of Bioactive Compounds in Natural Products Extracted from Plants in Cancer Treatment and Their Mechanisms Related to Anticancer Effects. Oxidative Medicine and Cellular Longevity, 2022.
5. Zhao, Y., Wang, C., & Goel, A. (2022). A combined treatment with melatonin and andrographis promotes autophagy and anticancer activity in colorectal cancer. Carcinogenesis, 43(3), 217-230.
6. Fulda, S., Jeremias, I., Steiner, H. H., Pietsch, T., & Debatin, K. M. (1999). Betulinic acid: a new cytotoxic agent against malignant brain-tumor cells. International journal of cancer, 82(3), 435-441.
7. Ahmad, M. Z., Rizwanullah, M., Ahmad, J., Alasmary, M. Y., Akhter, M. H., Abdel-Wahab, B. A., ... & Haque, A. (2022). Progress in nanomedicine-based drug delivery in designing of chitosan nanoparticles for cancer therapy. International Journal of Polymeric Materials and Polymeric Biomaterials, 71(8), 602-623.
8. Yogeeswari, P., & Sriram, D. (2005). Betulinic acid and its derivatives: a review on their biological properties. Current medicinal chemistry, 12(6), 657-666.
9. Kassi, E., Papoutsi, Z., Pratsinis, H., Aligiannis, N., Manoussakis, M., & Moutsatsou, P. (2007). Betulinicacid, a naturally occurring triterpenoid, demonstrates anticancer activity on human prostate cancer cells. Journal of Cancer Research and Clinical Oncology, 133(7), 493-500.
10. Yeh, C. T., Wu, C. H., & Yen, G. C. (2010). Betulinicacid, a naturally occurring triterpenoid, suppresses migration and invasion of human breast cancer cells by modulating c-Jun N-terminal kinase, Akt and mammalian target of rapamycin signaling. Molecular Nutrition and Food Research, 54(9), 1285-1295.
11. Eiznhamer, D. A., & Xu, Z. Q. (2004). Betulinic acid: a promising anticancer candidate. IDrugs: the investigational drugs journal, 7(4), 359-373.
12. Mullauer, F. B., Kessler, J. H., & Medema, J. P. (2010). Betulinic acid, a natural compound with potent anticancer effects. Anti-cancer drugs, 21(3), 215-227.

ISSN PRINT 2319 1775 Online 2320 7876

Research paper UGC CARE Listed (Group -I) Journal Volume 11,S Iss 3, Dec 2022

13. Kaur, H., Ahuja, M., Kumar, S., & Dilbaghi, N. (2012). Carboxymethyl tamarind kernel polysaccharide nanoparticles for ophthalmic drug delivery. International Journal of Biological Macromolecules, 50(3), 833-839.
14. Xu, L., Li, W., Sadeghi-Soureh, S., Amirsaadat, S., Pourpirali, R., & Alijani, S. (2022). Dual drug release mechanisms through mesoporous silica nanoparticle/electrospun nanofiber for enhanced anticancer efficiency of curcumin. Journal of Biomedical Materials Research Part A, 110(2), 316-330.
15. Van Aarssen, B. G. K., Cox, H. C., Hoogendoorn, P., & De Leeuw, J. W. (1990). A cadinene biopolymer in fossil and extant dammar resins as a source for cadinanes and bicadinanes in crude oils from South East Asia. Geochimica et Cosmochimica Acta, 54(11), 3021-3031.
16. Pfister, C. U., Martoni, A., Zamagni, C., Lelli, G., De Braud, F., Souppart, C., ... & Hornberger, U. (2001). Effect of age and single versus multiple dose pharmacokinetics of letrozole (Femara®) in breast cancer patients. Biopharmaceutics & drug disposition, 22(5), 191-197.
17. Smith, I., Yardley, D., Burris, H., De Boer, R., Amadori, D., McIntyre, K., ... & O'Shaughnessy, J. (2017). Comparative efficacy and safety of adjuvant letrozole versus anastrozole in postmenopausal patients with hormone receptor-positive, node-positive early breast cancer: final results of the randomized phase III Femara versus Anastrozole Clinical Evaluation (FACE) trial.
18. Gardin, G., Fornasiero, A., Romieu, G., Buzzi, F., Chaudri, H. A., & Lassus, M. (1998). Long duration of response with letrozole 2.5 mg (Femara®) in two trials in postmenopausal women with advanced breast cancer after anti-estrogen therapy. European Journal of Cancer, 34, S13-S14.
19. Moss, R. W. (2004). The war on cancer; Femara takes the cancer world by storm--Part 1. Townsend Letter for Doctors and Patients, (246), 34-36.
20. Ellis, M., & Ma, C. (2007). Femara® and the future: tailoring treatment and combination therapies with Femara. Breast cancer research and treatment, 105(1), 105-115.
21. Sethi, N., Bhardwaj, P., Kumar, S., & Dilbaghi, N. (2019). Development and Evaluation of Ursolic Acid Co-Delivered Tamoxifen Loaded Dammar Gum Nanoparticles to Combat Cancer. Advanced Science, Engineering and Medicine, 11(11), 1115-1124.
22. Kedare, S. B., & Singh, R. P. (2011). Genesis and development of DPPH method of antioxidant assay. Journal of food science and technology, 48(4), 412-422.
23. Plumb, J. A. (2004). Cell sensitivity assays: the MTT assay. In Cancer cell culture (pp. 165-169). Humana Press.

ISSN PRINT 2319 1775 Online 2320 7876

Research paper UGC CARE Listed (Group -I) Journal Volume 11,S Iss 3, Dec 2022

24. Jyothi, N. V. N., Prasanna, P. M., Sakarkar, S. N., Prabha, K. S., Ramaiah, P. S., & Srawan, G. Y. (2010). Microencapsulation techniques, factors influencing encapsulation efficiency. Journal of microencapsulation, 27(3), 187-197.
25. Dufort, S., Sancey, L., & Coll, J. L. (2012). Physico-chemical parameters that govern nanoparticles fate also dictate rules for their molecular evolution. Advanced Drug Delivery Reviews, 64(2), 179-189.
26. Yao, L., Ou, Z., Luo, B., Xu, C., & Chen, Q. (2020). Machine learning to reveal nanoparticle dynamics from liquid-phase TEM videos. ACS central science, 6(8), 1421-1430.
27. Ou, H., Cheng, T., Zhang, Y., Liu, J., Ding, Y., Zhen, J., ... & Shi, L. (2018). Surface-adaptive zwitterionic nanoparticles for prolonged blood circulation time and enhanced cellular uptake in tumor cells. Acta Biomaterialia, 65, 339-348.
28. Song, Ju, et al. "Development and characterisation of Betulinicacid nanocrystals without stabiliser having improved dissolution rate and in vitro anticancer activity." Aaps Pharmscitech 15.1 (2014): 11-19.
29. Kumari, A., Yadav, S. K., Pakade, Y. B., Singh, B., & Yadav, S. C. (2010). Development of biodegradable nanoparticles for delivery of quercetin. Colloids and Surfaces B: Biointerfaces, 80(2), 184-192.
30. Khuroo, T., Verma, D., Talegaonkar, S., Padhi, S., Panda, A. K., & Iqbal, Z. (2014). Topotecan–tamoxifen duple PLGA polymeric nanoparticles: investigation of in vitro, in vivo and cellular uptake potential. International journal of pharmaceutics, 473(1-2), 384-394.
31. Song, J., Wang, Y., Song, Y., Chan, H., Yang, X. et al. Development and characterisation of Betulinicacid nanocrystals without stabiliser having improved dissolution rate and in vitro anticancer activity. AAPS PharmSciTech, 15(1), 11-19 (2014).
32. Molyneux, P. (2004). The use of the stable free radical diphenylpicrylhydrazyl (DPPH) for estimating antioxidant activity. Songklanakarin Journal of Science and Technology, 26(2), 211-219.
33. Dahiya, S., Rani, R., Kumar, S., Dhingra, D., & Dilbaghi, N. (2017). Chitosan-gellan gum bipolymeric nanohydrogels—a potential nanocarrier for the delivery of epigallocatechin gallate. BioNanoScience, 7(3), 508-520.
34. Kalyane, D., Raval, N., Maheshwari, R., Tambe, V., Kalia, K., & Tekade, R. K. (2019). Employment of enhanced permeability and retention effect (EPR): Nanoparticle-based precision tools for targeting of therapeutic and diagnostic agent in cancer. Materials Science and Engineering: C, 98, 1252-1276.

ISSN PRINT 2319 1775 Online 2320 7876

Research paper UGC CARE Listed (Group -I) Journal Volume 11,S Iss 3, Dec 2022

35. Siegler, E. L., Kim, Y. J., & Wang, P. (2016). Nanomedicine targeting the tumor microenvironment: Therapeutic strategies to inhibit angiogenesis, remodel matrix, and modulate immune responses. Journal of Cellular Immunotherapy, 2(2), 69-78.
36. Tammina, S. K., Mandal, B. K., Ranjan, S., & Dasgupta, N. (2017). Cytotoxicity study of Piper nigrum seed mediated synthesized SnO2 nanoparticles towards colorectal (HCT116) and lung cancer (A549) cell lines. Journal of Photochemistry and Photobiology B: Biology, 166, 158-168.
37. Barua, S., & Mitragotri, S. (2014). Challenges associated with penetration of nanoparticles across cell and tissue barriers: a review of current status and future prospects. Nano Today, 9(2), 223-243.
38. Gerlier, D., & Thomasset, N. (1986). Use of MTT colorimetric assay to measure cell activation. Journal of immunological methods, 94(1-2), 57-63.
39. V. Meerloo, J., Kaspers, G. J., & Cloos, J. (2011). Cell sensitivity assays: the MTT assay. In Cancer cell culture (pp. 237-245). Humana Press.

Figure 1. PSA image of BFDNPs

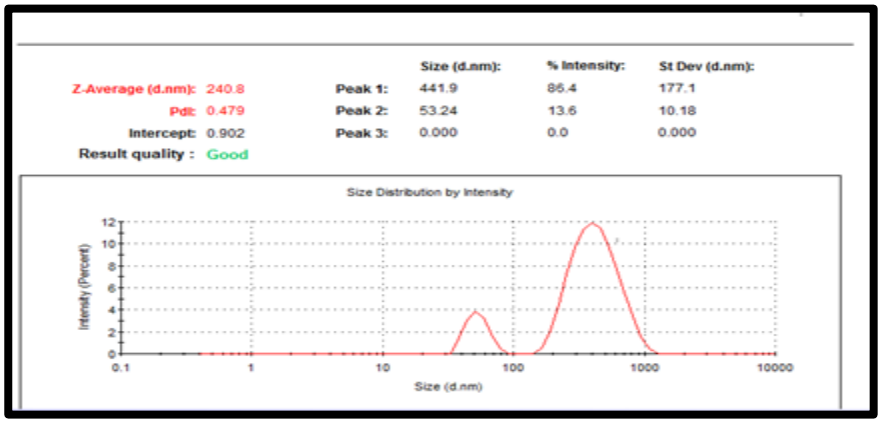

Figure 2. Zeta potential of BFDNPs

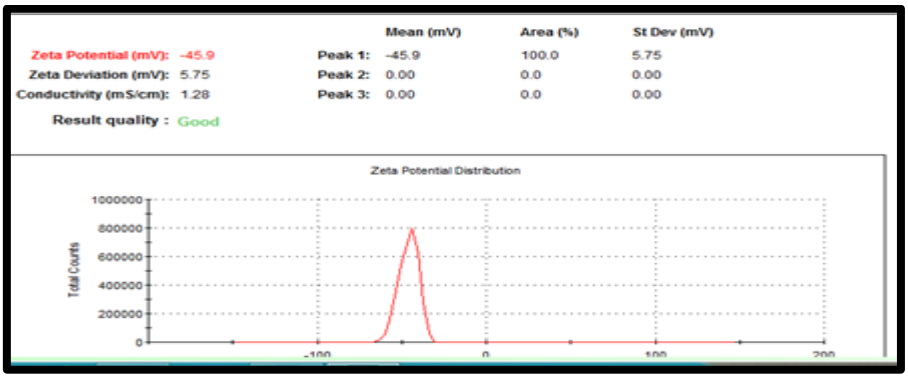

ISSN PRINT 2319 1775 Online 2320 7876

Research paper UGC CARE Listed (Group -I) Journal Volume 11,S Iss 3, Dec 2022

Figure 3: TEM image of BFDNPs

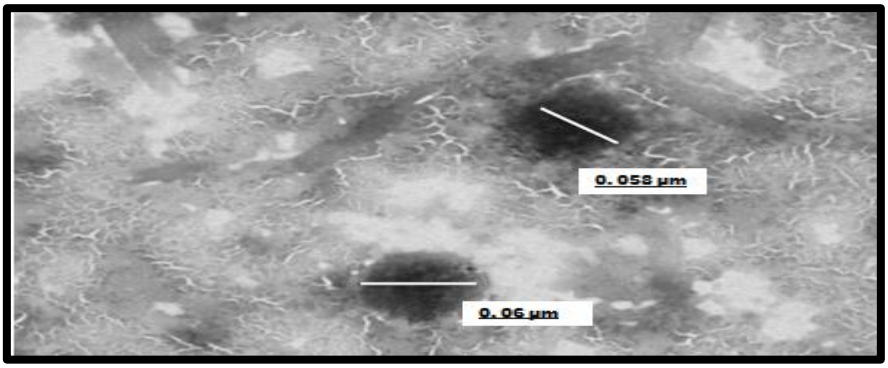

Figure 4. The FTIR spectra of pure drug(A)BA, (B)FEM, (C) Dammer gum,(D) BFDNP

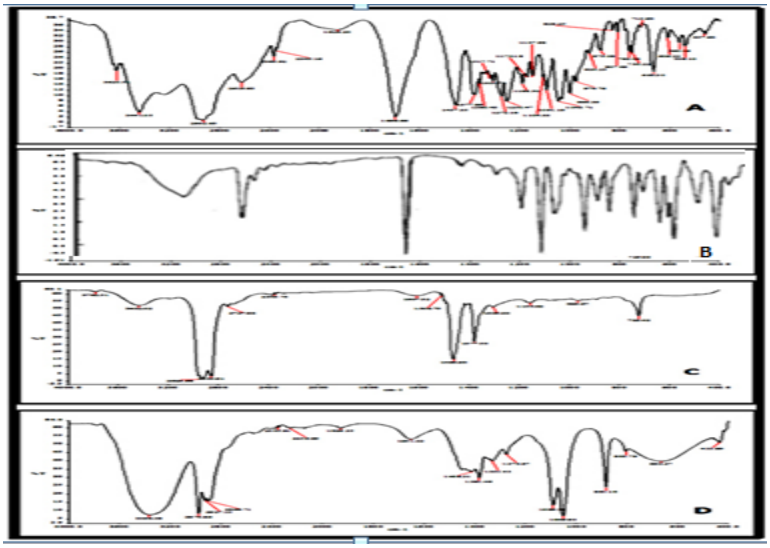

Figure 5. In-vitro release study

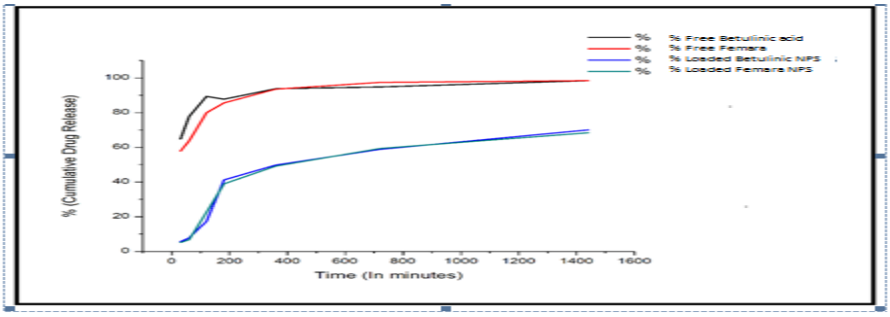

ISSN PRINT 2319 1775 Online 2320 7876

Research paper UGC CARE Listed (Group -I) Journal Volume 11,S Iss 3, Dec 2022

Figure 6. Antioxidant activity of UA, TAM and BFDNPs

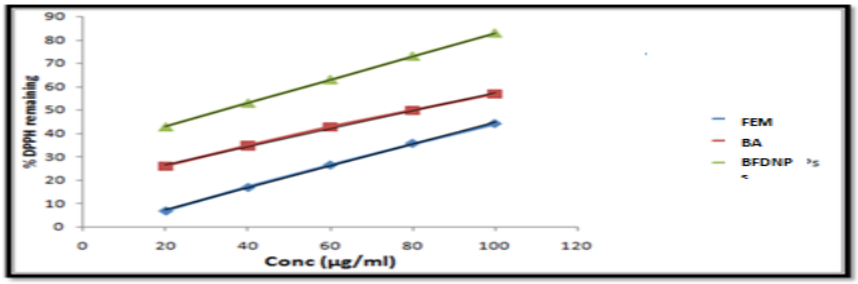

Table 1: IC50 values of BFDNPs along with standard drug Femara and Betulinic acid

Sample code	MCF-7	
	IC50	pIC50
Femara	5.48	-0.7387
Betulinic acid	26.66	-1.4258
BFDNPs	3.8	-0.5797

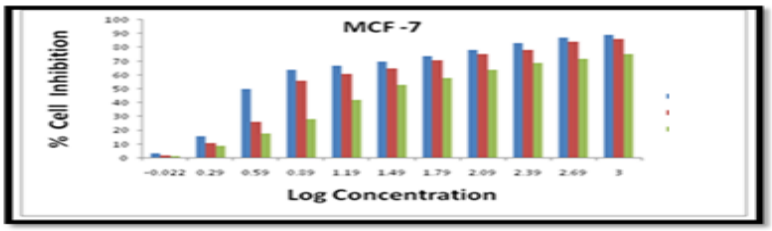

Figure 7. MTT assay on (A) MCF-7 cell line

ISSN PRINT 2319 1775 Online 2320 7876

Research paper UGC CARE Listed (Group -I) Journal Volume 11,S Iss 3, Dec 2022

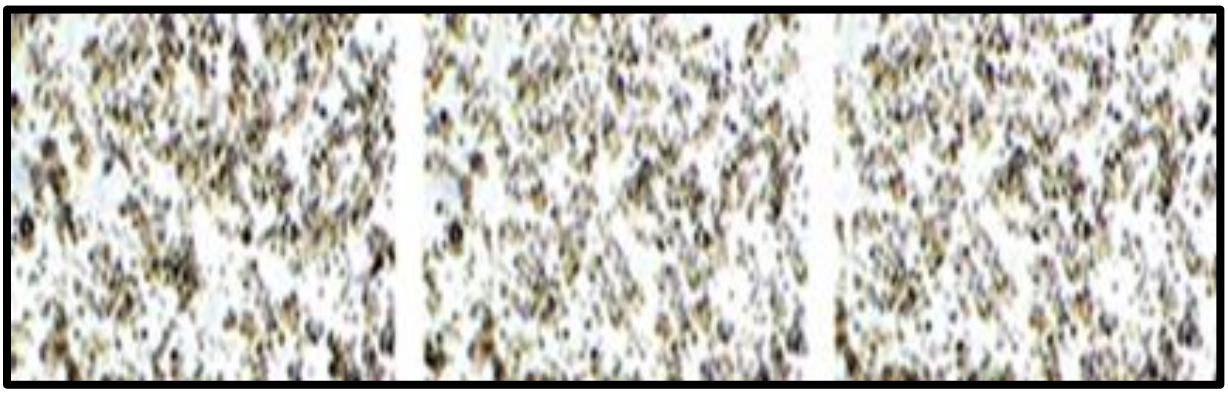

Figure 8. Optical microscope images of Cytotoxic effect of BA (B1),FEM (F1) and BFDNPs (N1), MCF-7 cell lines after 24 h.

B1 F1 N1